Supplementary information for:
Post-Earthquake Fold Growth Imaged With InSAR

Simon Daout[1*], Barry Parsons[1], Richard Walker[1]

[1] COMET, Department of Earth Sciences, University of Oxford, UK

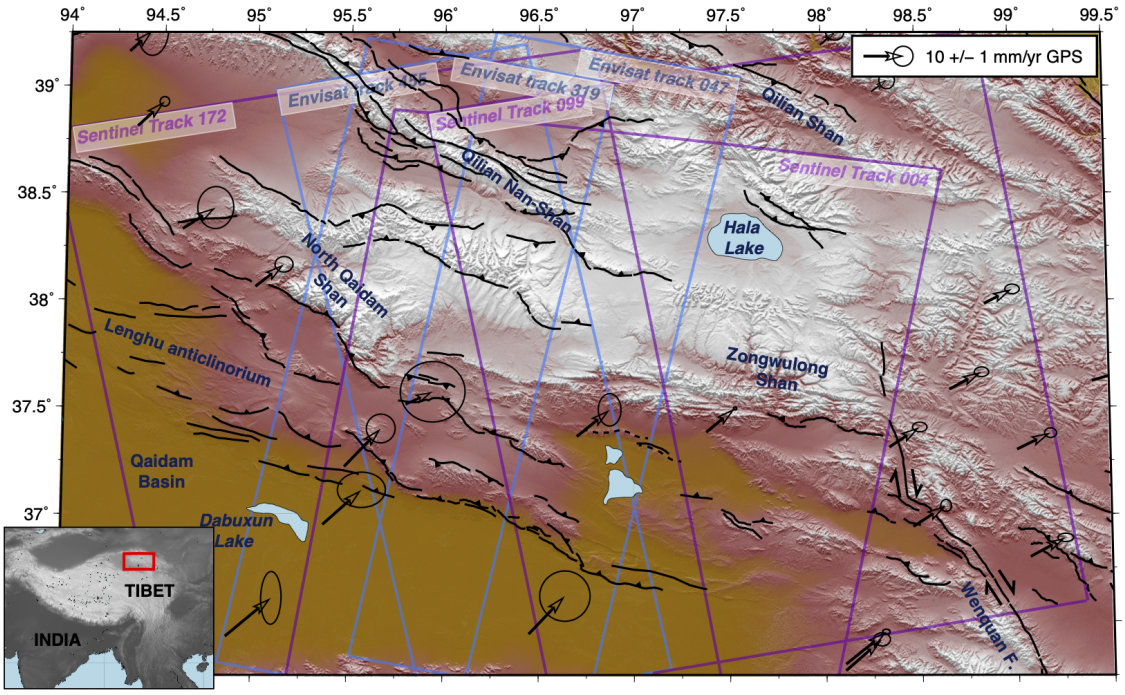

Figure S1: Surface traces of the 3 overlapping Envisat tracks (descending tracks 319, 047 and ascending track 455) and 3 overlapping Sentinel tracks (descending tracks 004 and ascending tracks 172 and 099) used in this study. Black arrows show the average GPS velocities relative to Eurasia (Wang et al., 2017). Topography is from the SRTM 30 m hill-shaded Digital Elevation Model.

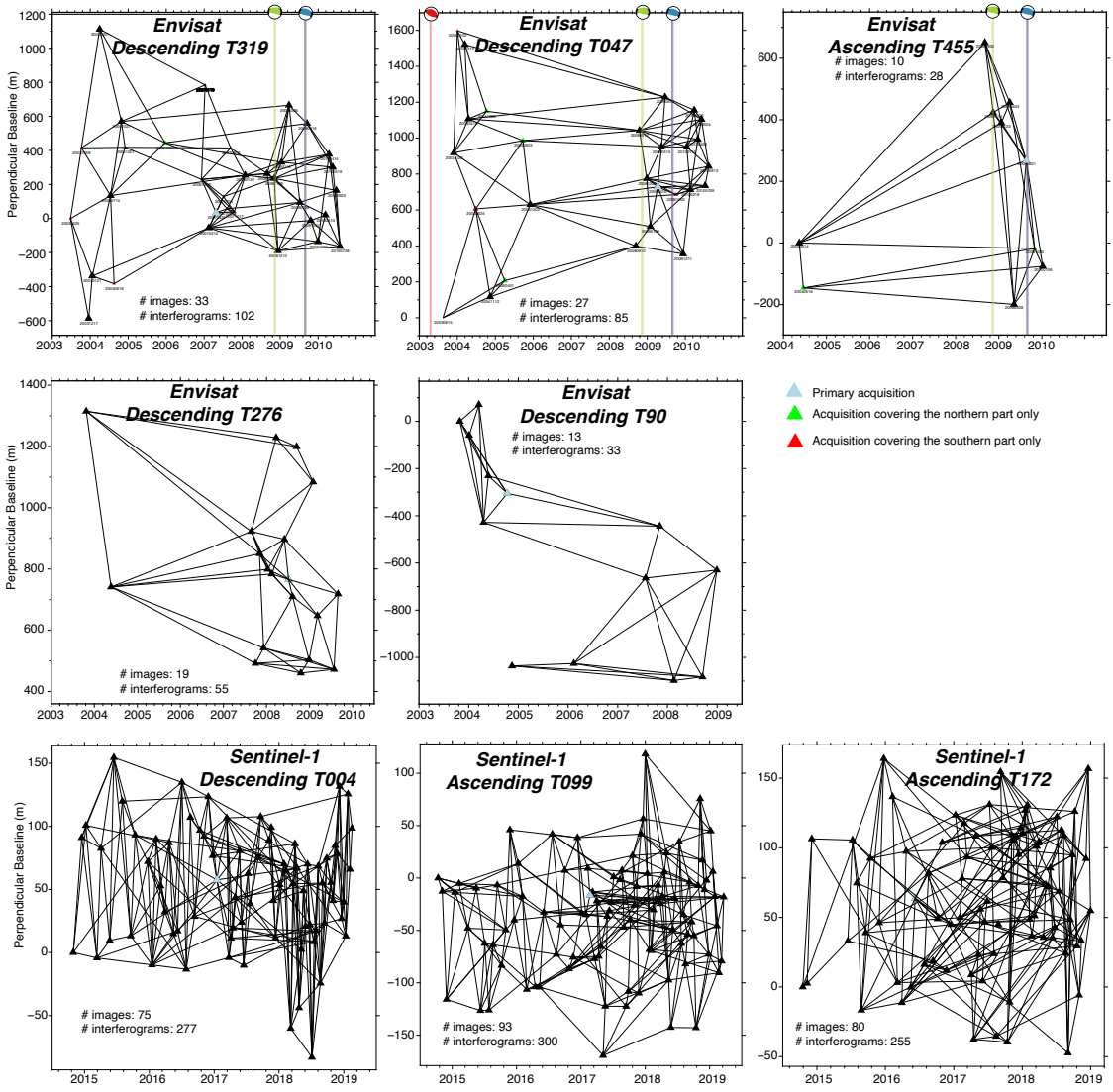

Figure S2: Computed interferograms for the three Envisat and three Sentinel-1 tracks. Triangles are SAR acquisitions with sizes and colors according the their spatial extent: black triangles for full coverage, green triangles for images covering the northern part of the track only, and red colors for images covering the southern part only. The reference images are shown with blue triangles.

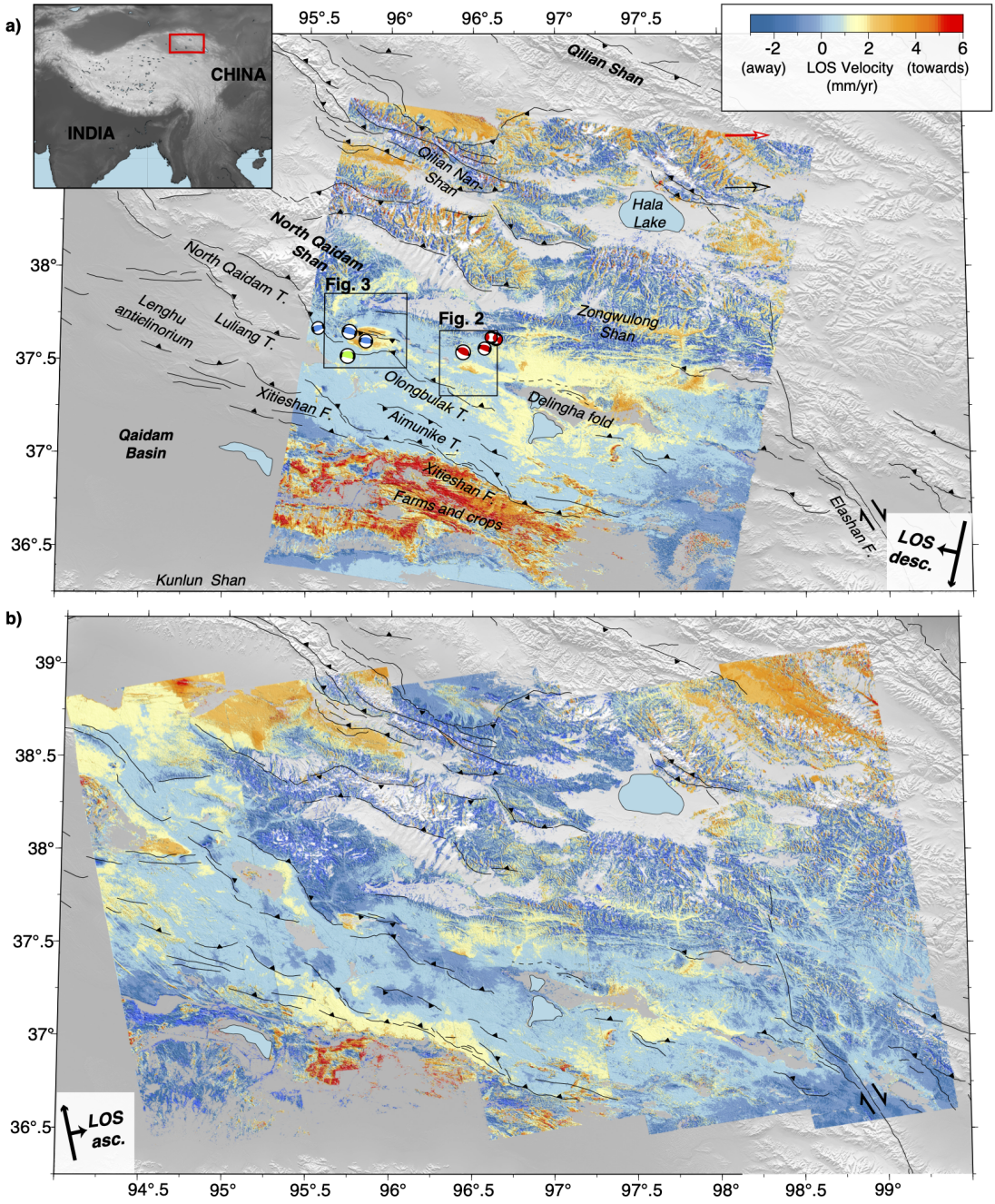

Figure S3: Line-of-Sight (LOS) velocity maps of the Sentinel-1 descending track 004 (a) and the two Sentinel-1 ascending tracks 099 and 172 (b), superimposed on shaded elevation, and focal mechanisms of the 8 Mw>5.2 events that occurred across the North Qaidam thrust system from 2003 to 2019. Positive motion is towards the satellite. Fault traces as in *Daout et al.* [2019]. Black boxes mark the areas of enlargements shown in Figs. 2, 3, 4 and 5 of the main text. Top left inset: regional setting and location of the area (red box).

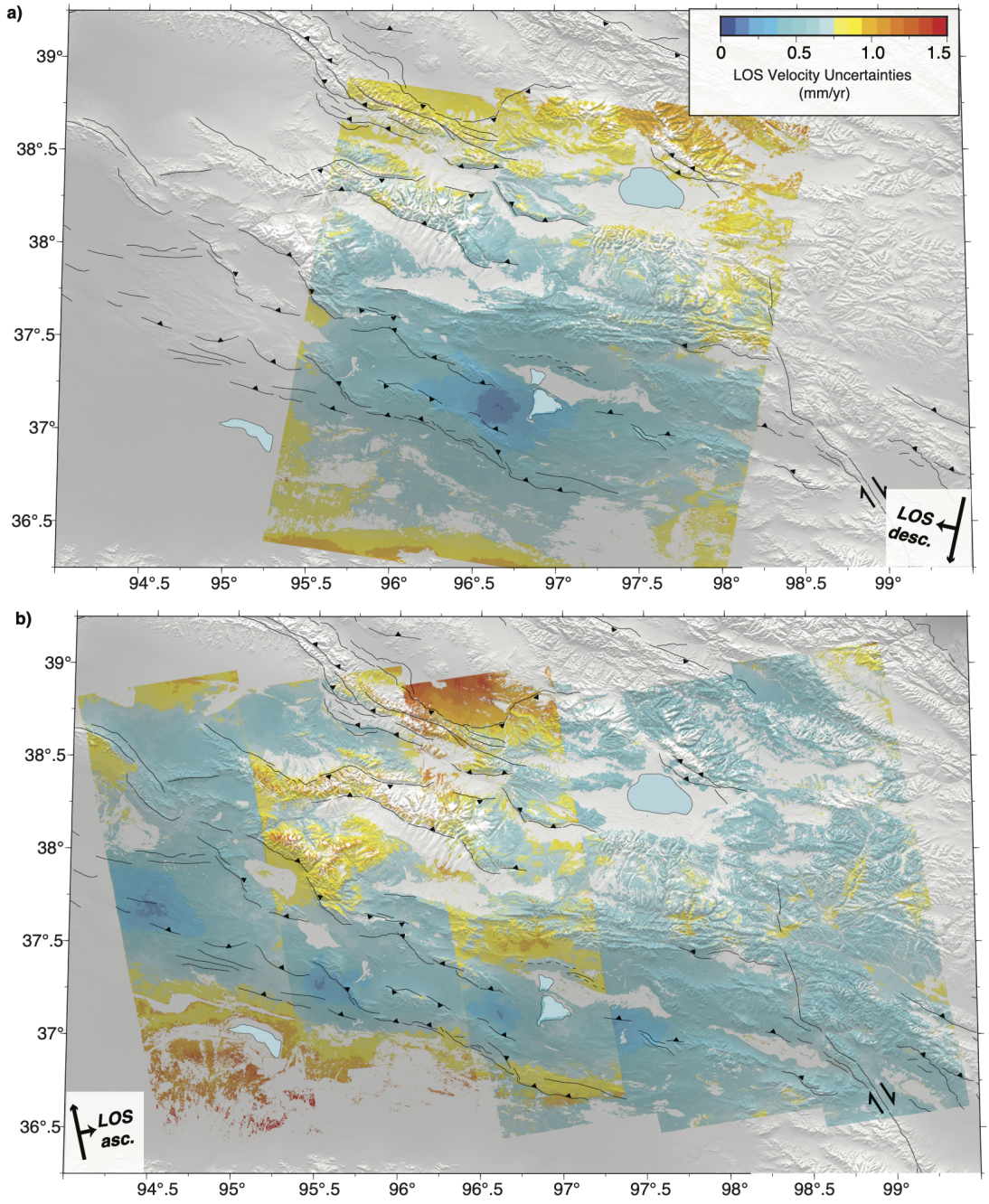

Figure S4: Line-of-Sight (LOS) velocity uncertainty maps of the Sentinel-1 descending track 004 (a) and the two Sentinel-1 ascending tracks 099 and 172 (b), superimposed on shaded elevation.

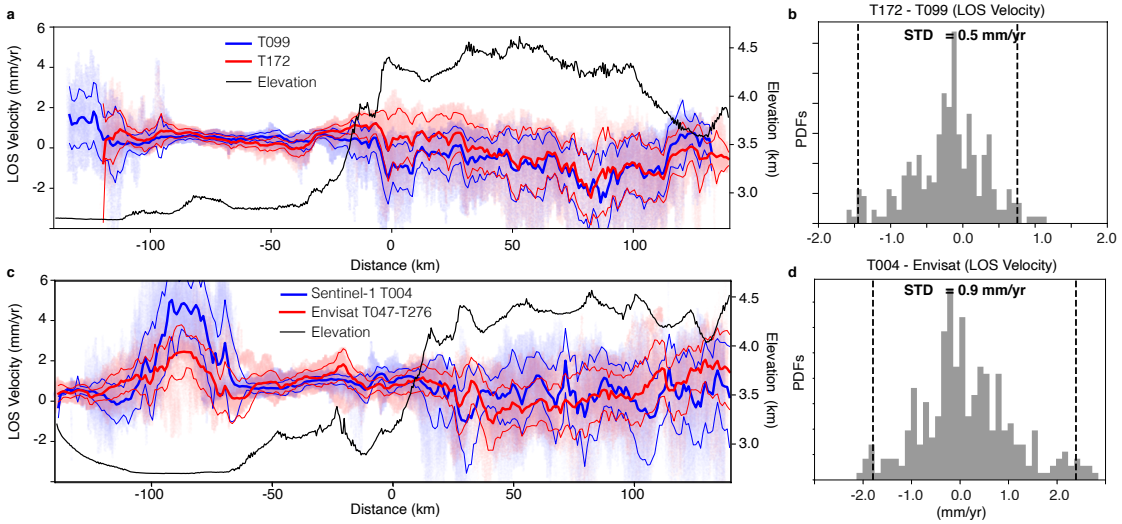

Figure S5: a: 280 km-long and 50 km-wide profile in the overlapping areas of the two ascending tracks 099 and 172. The thick blue and red lines correspond to the median in sliding windows of 1 km along profile, for track 099 and 172, respectively, while the thin lines correspond to the sliding windows standard deviations along profile. b: Histogram of differences between overlapping areas of the two ascending tracks with associated 95% intervals. c: Same as a) but for the 280 km-long and 50 km-wide profile of Fig. S4 in the overlapping areas of the Envisat descending tracks and Sentinel-1 descending track 004. d) Histogram of differences between overlapping areas of the two descending tracks with associated 95% intervals.

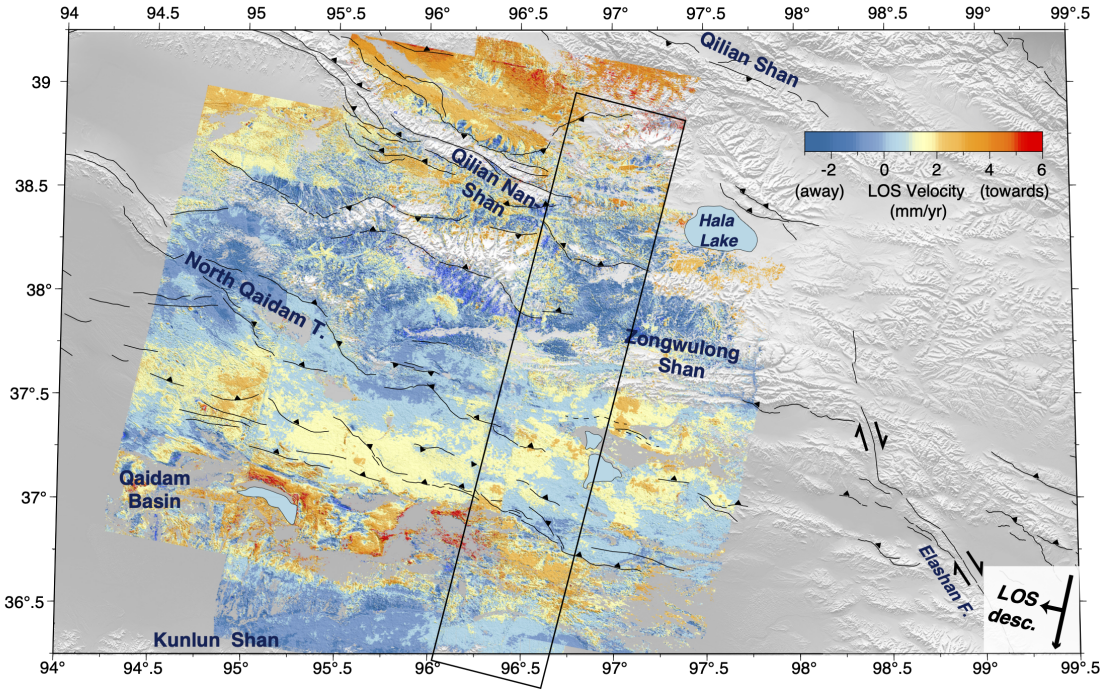

Figure S6: Line-of-Sight (LOS) velocity map of the four descending tracks 90, 319, 047, and 276 from Daout et al., 2019, corrected from post-seismic deformations with a parametric approach, with location of the profile of Fig. S3c.

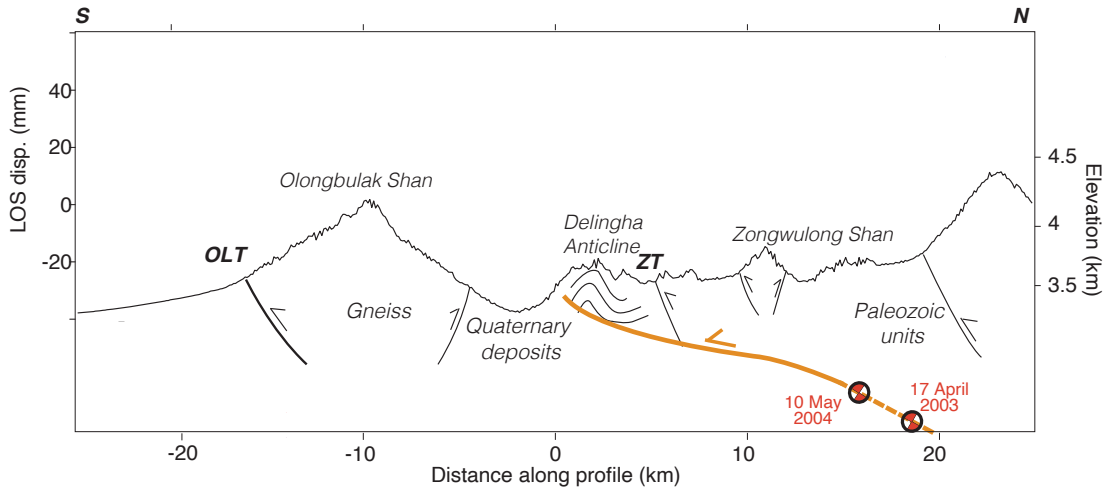

Figure S7: Interpreted structural cross-section sketch across the Olongbulak and Zongwulong ranges from *Daout et al.* [2019]. Orange line corresponds to the modeled post-seismic signal observed with Envisat across the Delingha anticline.

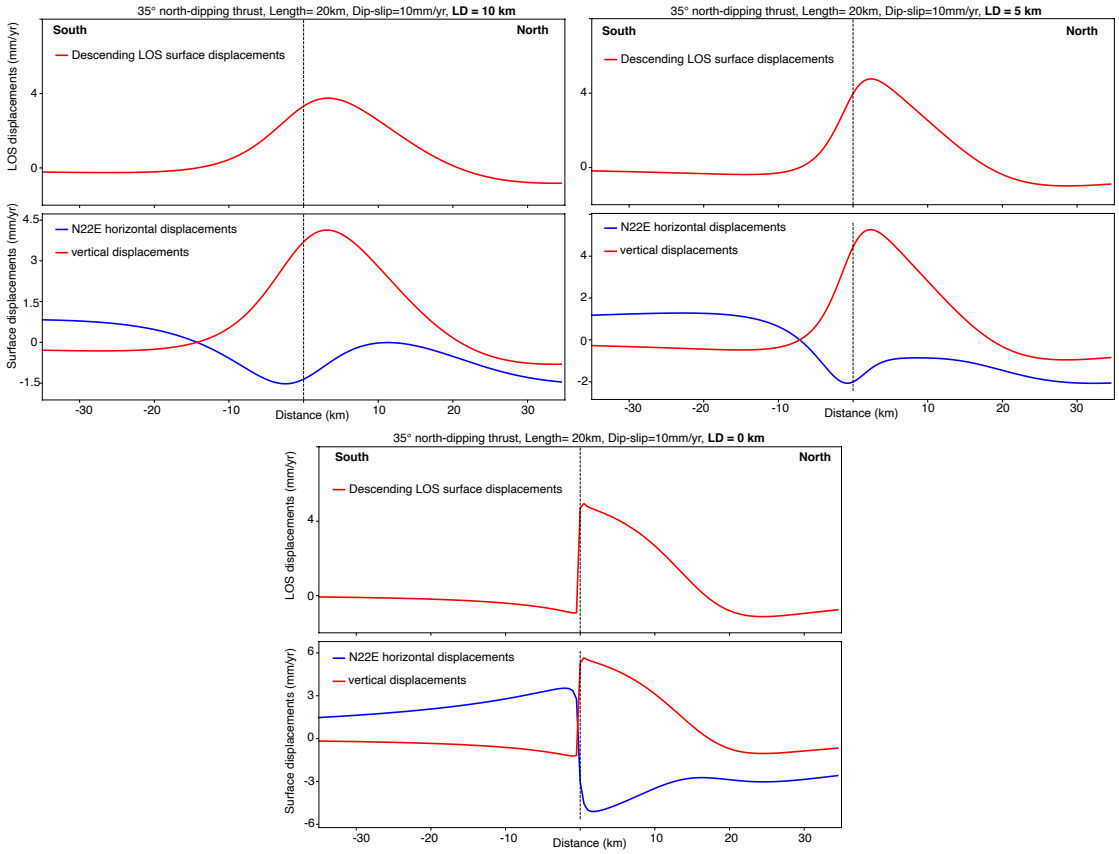

Figure S8: Forward models for one 35° north-dipping and 20 km-long edge dislocation embedded in an elastic half-space with variable locking depths (LD) (0 km, 5 km and 10 km).

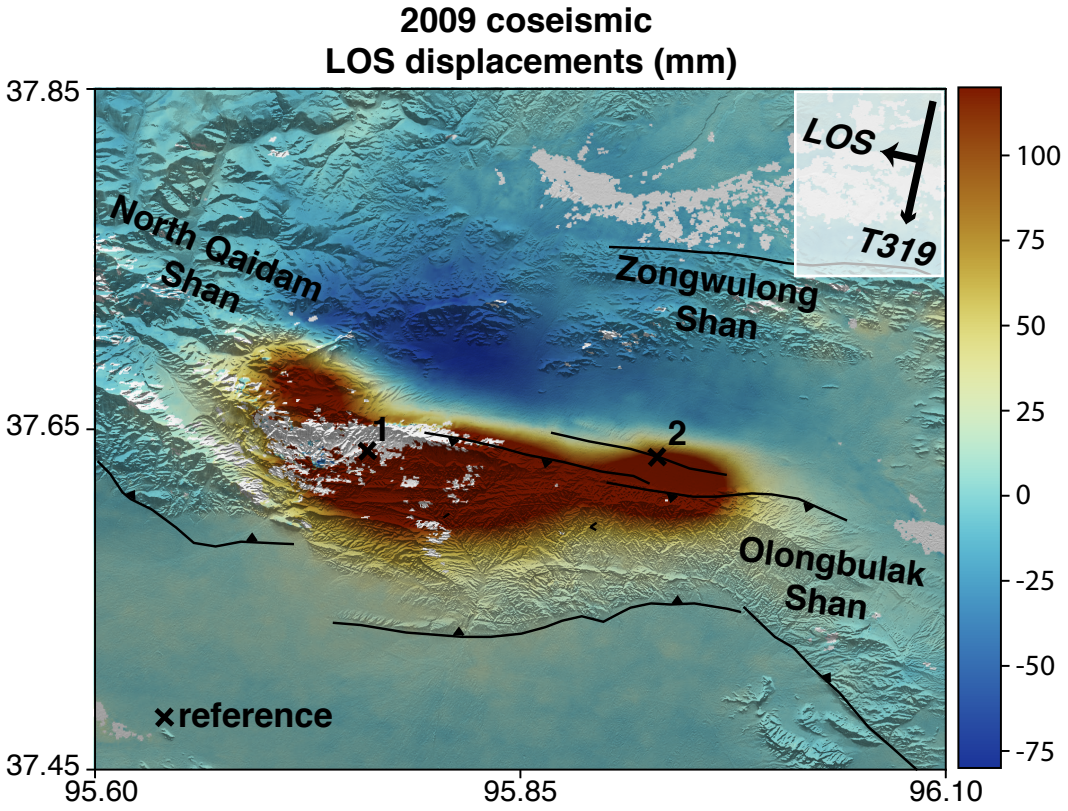

Figure S9: LOS surface displacements associated with the 2009 Haixi earthquake extracted from the parametric decomposition of track 319.

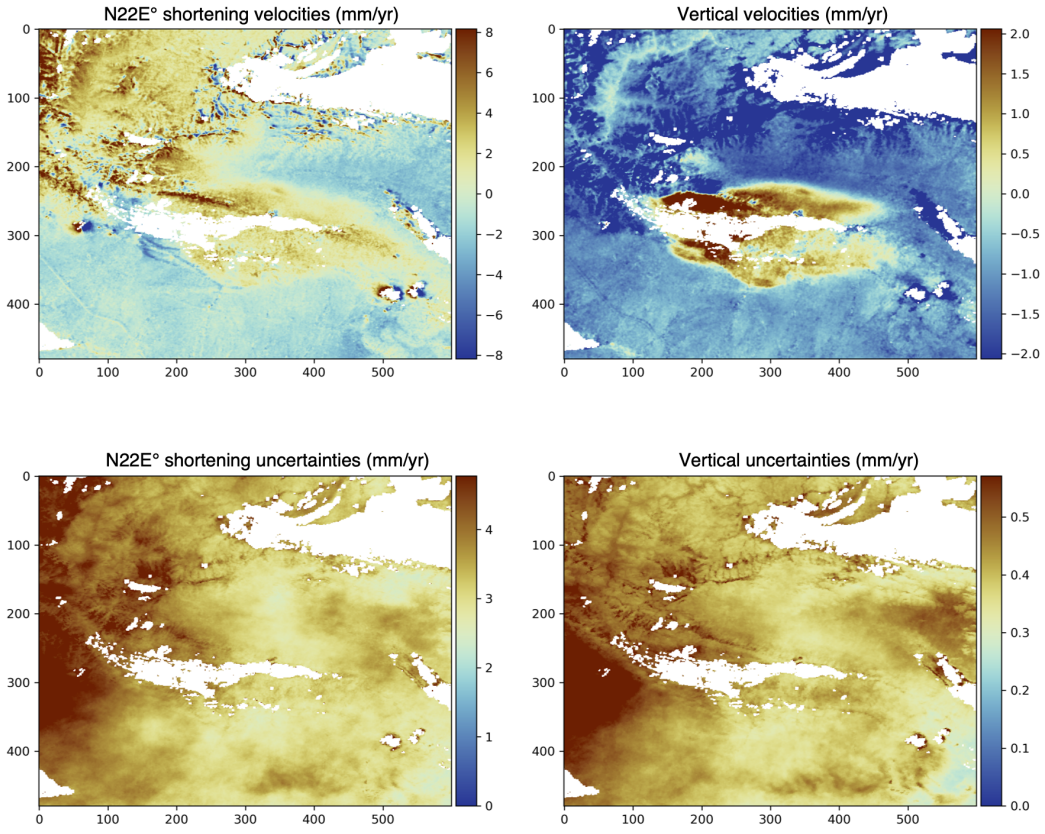

Figure S10: N22E shortening and vertical surface displacement velocities (top) with associated posterior uncertainties (bottom) of Fig. 4 in the main text (Haixi earthquakes area).

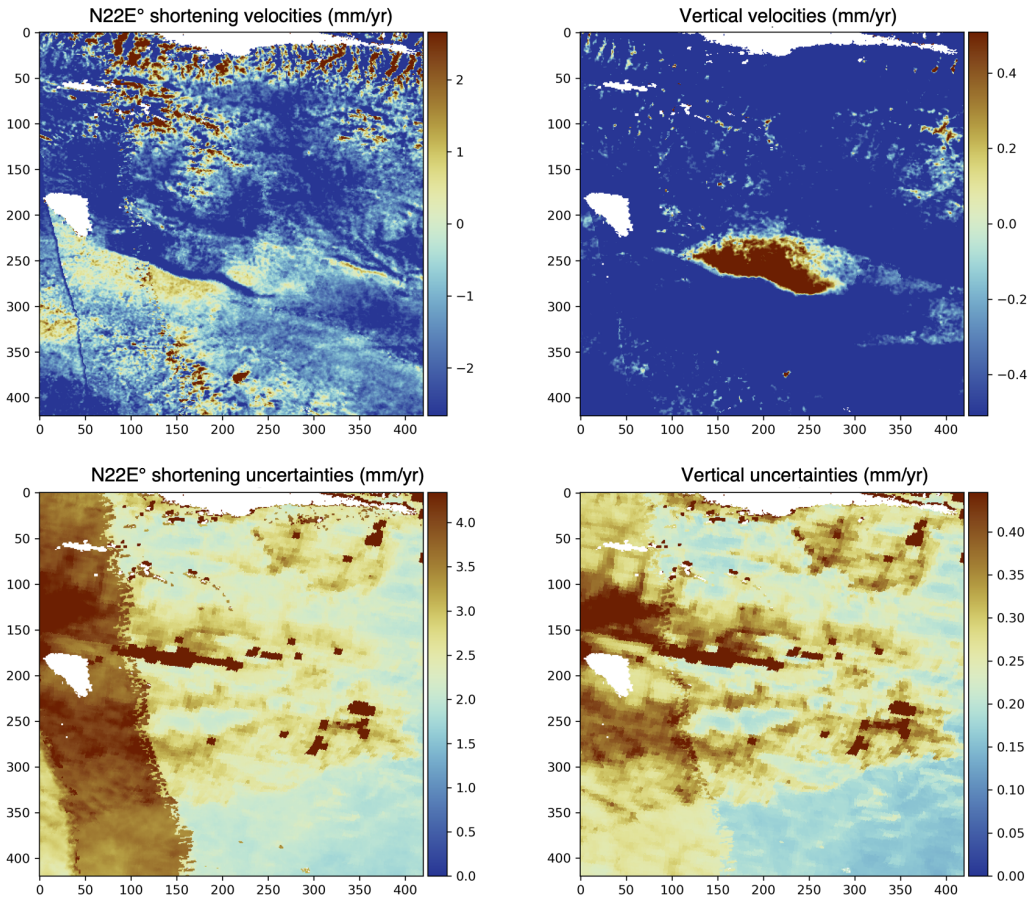

Figure S11: N22E shortening and vertical surface displacement velocities (top) with associated posterior uncertainties (bottom) of Fig. 5 in the main text (Delingha area).

References

Daout, S., H. Sudhaus, T. Kausch, A. Steinberg, and B. Dini, Interseismic and postseismic shallow creep of the North Qaidam Thrust faults detected with a multitemporal InSAR analysis, *Journal of Geophysical Research: Solid Earth*, *124*(7), 7259–7279, 2019.